https://doi.org/10.5194/acp-2021-158
Preprint. Discussion started: 26 March 2021

Atmospheric Chemistry and Physics
Discussions

Shift in seasonal snowpack melt-out date due to light-absorbing particles at a high-altitude site in Central Himalaya

Johan Ström[1], Jonas Svensson[2,3], Henri Honkanen[4], Eija Asmi[2], Nathaniel B. Dkhar[5], Shresth Tayal[5,6], Ved P. Sharma[5,6], Rakesh Hooda[2], Outi Meinander[2], Matti Leppäranta[4], Hans-Werner Jacobi[3], Heikki Lihavainen[7,2], Antti Hyvärinen[2]

1 Department of Environmental Science, Stockholm University, Stockholm, Sweden

2 Atmospheric Composition Research, Finnish Meteorological Institute, Helsinki, Finland

3 Université Grenoble-Alpes, CNRS, IRD, INP-G, IGE, Grenoble, 38000, France

4 Institute for Atmospheric and Earth System Research, Faculty of Science, University of Helsinki, Helsinki, Finland

5 The Energy and Resource Institute, (TERI) New Delhi, India

6 TERI School of Advanced Studies (TERI SAS), New Delhi, India

7 Svalbard Integrated Arctic Earth Observing System, Longyearbyen, Norway

Correspondence to: jonas.svensson@fmi.fi

Abstract

Snow darkening by deposited light-absorbing particles (LAP) has the potential to accelerate snowmelt and shift the snow melt-out date. Here we investigate the sensitivity of the seasonal snow cover duration to changes in LAP at a high altitude valley site in the Central Himalayas, India. First, the variation of the albedo of the seasonal snow was emulated using two seasons of automatic weather station (AWS) data and applying a constant, but realistic deposition of LAP to the snow. Then, the number of days with snowmelt were evaluated based on the estimated net energy budget of the seasonal snow cover and the derived surface temperature. The impact on the energy budget by LAP combined with the melt-day analysis resulted in very simple relations to determine the contribution of LAP to the number of days with snowmelt of the seasonal snow in Himalaya. Above a concentration of 1 ng g^{-1} (Elemental Carbon equivalent, EC_{eq}, which in this study includes EC and the absorption equivalent EC contribution by other light absorbing particles, such as mineral dust) in new snow, the number of days with snowmelt can be estimated by; $days = 0.0109(\log(EC_{eq})+1)PP \pm 0.0033(\log(EC_{eq})+1)PP$, where PP is the seasonal precipitation in mm snow water equivalent. A change in EC_{eq} by a factor of two corresponds to about $\frac{1}{3}$ of a day per 100 mm precipitation. Although the change in the number of days with melt caused by the changes in EC_{eq} is small, the estimated total change in the snow melt-out date by LAP can be significant. For our realistic base case scenario for the Sunderdhunga Valley, Central Himalayas, India, of EC_{eq}=100 ng g^{-1} and PP=400 mm, this yields in an advancement of the melt-out date of about 13 days.

https://doi.org/10.5194/acp-2021-158
Preprint. Discussion started: 26 March 2021

Atmospheric Chemistry and Physics Discussions

1. Introduction

Seasonal snow cover in the Himalaya is an integral component of the regional hydrological cycle, with the timing of the melting phase being crucial for the supply of fresh water with growing importance at increasing altitudes (e.g. Armstrong et al., 2018; Mimeau et al., 2019). Replacing a bright snow surface for a darker soil surface drastically changes the local climate. The albedo of snow has a key role in the energy balance of the snow pack, and may be the main controller of snow melt (Cuffey & Paterson, 2010). Strongly dependent on the microphysical properties of snow (e.g. snow liquid water content, grain size, and shape; Aoki et al., 2003), the albedo is also affected by the presence of light-absorbing particles (LAP) (Warren & Wiscombe, 1980). Originating mostly from anthropogenic emissions, LAP can be transported from distant source regions before being mixed with snow, making this factor particularly interesting with regards to a potential human influence on the regional climate and hydrological cycle. The two main components of LAP in the Himalaya are mineral dust (MD) and light-absorbing carbonaceous particles. Whereas MD can be regarded as having mainly natural sources, black or brown carbon (BC, BrC) are mainly attributed to human activities associated with the combustion of biomass and fossil fuels, although natural wild-fires can also be a very significant source of BC and BrC.

A common technique to analyze carbonaceous particles in snow is to use a thermo-optical method that yields the mixing ratio of elemental carbon (EC) to the melted snow volume/mass, or snow water equivalent (SWE) commonly expressed as, µg L^{-1}, ng g^{-1}, or ppb_w (e.g. Forsström et al., 2009; Ming et al., 2008). Because EC is the main light absorbing component of BC, these acronyms are sometimes used interchangeably in the literature, although BC most commonly refers to optically detected LAP (see e.g. Petzold et al., 2013). In addition, the refractory component of BC (rBC) in snow can be determined (e.g. Schwarz et al., 2012). Here we work with EC or the equivalent EC (EC_{eq}). The latter is the sum of EC and the absorption equivalent EC contribution by MD or other light absorbing components (as measured in Svensson et al. 2018; 2021).

Snow darkening by BC in the Himalayan cryosphere has been shown to significantly vary regionally (e.g. Gertler et al., 2016). The other main LAP constituent, MD, was recently identified as the dominating light absorber in the snow above 4000 m altitude for High Mountain Asia (Sarangi et al. 2020). In contrast, Schmale et al. (2017) reported BC as the main particle absorber in measurements of glacier snow samples from Kyrgyzstan, Central Asia. The authors also presented a model to estimate the fraction of snowmelt attributable to LAP. The model took into account the absorptivity of the snow and the amount of incoming shortwave radiation, as well as the number of days with a temperature above 0 °C, to estimate a summer snowmelt rate increase of up 6.3% due to LAP. This model has been applied over the Tibetan plateau with different SWE and shortwave radiation scenarios (220, 270, and 310 W m^{-2}) for BC and MD (Zhang et al., 2018). That study present a range of 1.3 - 1.8 days of reduction in average snow cover duration (SCD) for a SWE of 40 mm due to BC and MD, whereas for a 100 mm SWE the SCD reduction was 3.1 - 4.4 days. It is further concluded that the reductions in SCD is mainly because of BC, and not MD, for that area. Similarly the model was used in Northern Xinjiang, China, with different SWE and shortwave radiation scenarios for BC and MD, shortening the SCD in

https://doi.org/10.5194/acp-2021-158
Preprint. Discussion started: 26 March 2021

the range of 1.4 ± 0.6 to 6.1 ± 3.4 days (Zhong et al., 2019). As a comparison, a different approach to estimate the reduced snow cover was presented by Ménégoz et al. (2014). Utilizing a climate-chemistry global model to approximate the effect from BC deposition on the Himalayan snow cover, they found an annual reduction in SCD by 1 to 8 days. The authors conclude that the low precipitation rates of snow over the Tibetan Plateau contribute to the low number, while anthropogenic BC is expected to have a larger effect in the mountain ranges (Himalaya, Karakoram, Hindu-Kush).

Common for the studies summarized above is that they are based on an extensive dataset and/or complex numerical models, and that the results are not generalized. Here we study the influence by LAP on the seasonal snow cover duration with a different approach, attempting to reduce the information needed and at the same time generalizing the results. We use two seasons of automatic weather station (AWS) data from the Sunderdhunga Valley at about 4700 m altitude in central Himalaya, as well as observations on LAP in the glacier snow from the same valley (Svensson et al., 2021), to investigate the sensitivity of seasonal snow cover duration to changes in EC_{eq}. Through analysis of these two seasons and a series of assumptions and simplifications, the complex system of LAP and albedo reduction is condensed down into a dependence of only a few variables. With these simplified relations we attempt to answer the question: what is the contribution to the number of days with snowmelt from a given change of LAP in the seasonal snow for the study region?

The analysis is conducted in two main sections. Section 3 presents how a parametric description of the daily variation in albedo is formulated (with taking into account LAP and ground albedo) and how that albedo compares to the observed albedo. Section 4 presents how the data is analyzed with respect to the number of days with melt associated with each season. The results are combined into simple relations to estimate the influence on the contribution of LAP to the number of days with snowmelt, based on the LAP content in the snowpack and the seasonal precipitation.

2. *Observations*

2.1 Automatic weather station

The AWS observations are from the immediate vicinity (~100 m) of the glacier ablation zone of Durga Kot glacier in the Sunderdhunga valley, northern India, further described in Svensson et al. (2021). Two seasonal snow cover periods are utilized here (indicated by arrows in Figure 1), lasting between 6 February 2016 and 22 May 2016 (season 1), and between 24 December 2016 and 1 June 2017 (season 2). The AWS is equipped with instrumentation for air temperature (T_a), relative humidity (RH) (HC2S3-L Temperature and relative humidity probe manufactured by Rotronic, with 41303-5A Radiation shield), broadband shortwave radiation upward and downward (SW_u, SW_d) and longwave radiation upward and downward (LW_u, LW_d) (CNR4 Four-component net radiometer manufactured by Kipp & Zonen), snow depth (SD) (Campbell Scientific SR50A-L Ultrasonic Distance Sensor), wind speed (U), and wind direction (not used in this paper) (05103-L Wind monitor manufactured by R. M. Young). Data was logged every 10 minutes and screened for inconsistencies, which may arise, for example, from snow covering the sensors. Subsequently, the data was averaged over each day, expect

https://doi.org/10.5194/acp-2021-158
Preprint. Discussion started: 26 March 2021

for albedo and SD which are based on daily median values. The time series of albedo and SD are presented in Figure 1.

Based on LW_u and assuming unit emissivity of snow, the Stephan-Boltzmann's Law (supplement equation 1) is used to calculate a representative surface temperature (T_s). Using a lower emissivity would result in higher T_s, but will not affect the interpretation of the data. Precipitation was not explicitly measured at this location, but is estimated similar to the method described in Svensson et al. (2021), yielding an estimate of the amount of precipitation in mm SWE (PP). The positive changes in snow depth (SD^+) are integrated over the periods in question and the density of the new snow is assumed to be 100 kg m^{-3} (Helfricht, et al., 2018). The estimated total PP for season 1 and season 2 are 290 and 460 mm, respectively. The measured AWS variables recorded during the two seasons are further presented in supplement Figure S1.

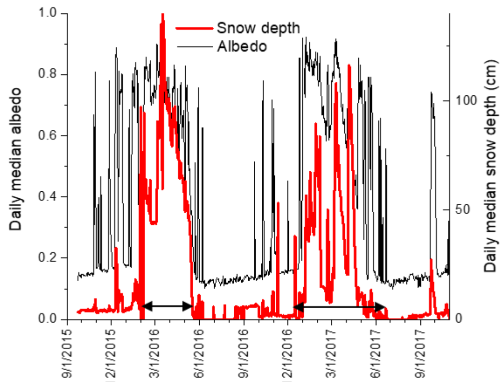

Figure 1. Daily median albedo and snow depth from 22 September 2015 to 31 October 2017. The period considered for the two seasonal snow covers are indicated with the black double arrow lines.

2.2 Light-absorbing particles

The basis for LAP in the snow for this study originates from observations reported in Svensson et al. (2021). They showed that LAP in young snow (interpreted as snow from the current winter season), sampled at Durga Kot and the neighboring Bhanolti glacier at a distance about 1-2 km due southwest from the AWS at about 5000 m altitude, can be described by a characteristic constant deposition of EC of about 50 µg m^{-2} PP^{-1}. In other words, each mm of precipitation contains an EC concentration of 50 ng g^{-1}. For both winter seasons the dry deposition of EC likely contributed small amounts to the overall deposition of EC as proposed in Svensson et al. (2021). Using a dry deposition velocity of BC of 0.3 mm/s (Emerson et al., 2018) and an atmospheric concentration of 0.3 µg m^{-3}, reported at the Nepal Pyramid station during the pre-monsoon (Bonasoni et al., 2010), the dry deposition can be estimated to contribute to EC by 845 µg m^{-2} and 1236 µg m^{-2} for season 1 and 2, respectively. Comparison to the EC wet deposition estimates for seasons 1 and 2: 14500 µg m^{-2} and 23000 µg m^{-2} (obtained by multiplying 50 µg m^{-2} with the PP of each season), suggests that EC dry deposition is on the order of 5-6% of the total EC deposition. The two analyzed seasons here represent the main precipitation

https://doi.org/10.5194/acp-2021-158
Preprint. Discussion started: 26 March 2021

Atmospheric Chemistry and Physics
Discussions

periods of the year for this site, further supporting the argument that dry deposition is not significant for our investigations.

3. Albedo parameterization

3.1 Effective grain size, pristine albedo and specific surface area of snow

For snow, the effective grain size (r_e) can be estimated by the ratio between volume and area according to

$$r_e = \frac{3}{\rho_i SSA} \quad (1)$$

Where ρ_i is the density of ice (910 kg m^{-3}), and SSA is the specific surface area of snow (m^2 kg^{-1}). The formulation proposed by Gardner and Sharp (2010) relates the albedo of pristine snow (a_p) to variations in SSA as

$$a_p = 1.48 - SSA^{-0.07} \quad (2)$$

where a_p is the albedo of pristine snow (i.e. without LAP) and SSA is given in (cm^2 g^{-1}). Liquid water in snow influence the albedo indirectly by enhancement of r_e and filling voids between the snow crystals (Colbeck, 1979). Changes in r_e, SSA and a_p are often parameterized using variations of summed daily maximum temperatures since the last snow fall to capture the metamorphism of the snow over time (e.g. Winter, 1993; Brock et al., 2000). We are interested in a relation that directly connects our AWS observations to the grain size of pristine snow. Therefore, we explore to diagnose SSA for pristine snow as function of T_a or T_s based on our own data set. This is done by grouping the data in one degree temperature bins using all available data (from 22 September 2015 to 31 October 2017). For each temperature bin, the maximum albedo was identified and the corresponding SSA was calculated with eq. 2. The logarithm of the SSA is presented in supplement Figures S2a and S2b as a function of temperature. The maximum albedo for each temperature bin is assumed to represent snow that is the least effected by LAP and corresponds, thus, most closely to pristine conditions. The fitting was done to log(SSA) using bins with suitable data coverage (and/or snow cover), therefore excluding low and high temperature bins from the fits (see Figure S2). Calculations were made for both T_s and T_a, but the results proved to be very similar. For simplicity, further correlations are here presented mostly as function of T_a. The dependence of log(SSA) of air temperature can be written as

$$\log(SSA) = -5.92 \cdot 10^{-3} T_a - 0.193 T_a + 1.97 \quad (3)$$

where SSA is given in cm^2 g^{-1} and T_a in °C (the relation log (SSA) and T_s is provided in the supplement). For a given daily average temperature, equation 3 provides the estimated SSA of the brightest snow surface albedo based on two seasons of data. Those events are thought to occur for relatively young snow without significant influence from LAP. However, this empirical relation will provide the same albedo for young snow at a given daily temperature as for snow that fell at an earlier instance, but with a different temperature for a particular day. After the snow fell, the temperature either increased or decreased. Because eq. 3 only depends on the average temperature of the day, this memory effect is not captured by the parameterization (see additional reasoning in supplement).

https://doi.org/10.5194/acp-2021-158
Preprint. Discussion started: 26 March 2021

Atmospheric Chemistry and Physics Discussions

Through a combination of equations 3, 2, and 1, a projected value of the albedo of near pristine snow and effective grain size, can be derived as function of the air temperature. As T_a increases r_e increases, while a_p decreases.

3.2 Albedo reduction by LAP

With a value for a_p, the subsequent step is to introduce the albedo reduction due to LAP. The empirical relation proposed by Pedersen et al. (2015) is used for the scaling factor of pristine snow

$$y_\lambda = A - B\, x^C \tag{4}$$

Where A, B and C are wavelength dependent constants (provided in the supplement section 4). The variable x is

$$x = \sqrt{\overline{EC_{eq}} r_e} \tag{5}$$

where $\overline{EC_{eq}}$ is the average equivalent EC content (EC plus other LAP) in (ng g^{-1}) in the surface snow and r_e is given in (µm). This parameterization is designed for EC_{eq} concentrations between 1 and 400 ng g^{-1}, but Svensson et al. (2016) has shown that it can be used with reasonable result at significantly higher concentrations.

As stated above, in this study the EC_{eq} content includes the albedo reduction from both EC and the equivalent content from other absorbers such as MD, BrC or other light absorbing organic carbon. The concentration or mixing ratios of these species are not know as a function of time a priori. For our measurement site at Sunderdhunga, Svensson et al. (2021) presented evidence of a rather constant mixing ratio of 50 ng g^{-1} of EC in fresh snow and a contribution to light absorption by MD of about 50 %. Thus, we assume that EC_{eq} is equal to two times EC. This estimate of EC_{eq}=100 ng g^{-1} is used as our base case throughout this study. An additional assumption is that while snow sublimates and melts, LAP preferentially stays near the surface, as previously observed (e.g. Doherty et al., 2013; Svensson et al., 2016; Xu et al., 2012) in some characteristic depth *d* (mm) expressed in terms of SWE. The representative or average $\overline{EC_{eq}}$ is then related to the variation in SD according to

$$\overline{EC_{eq}}_n = \left(EC_{eq} d + \sum_{i=1}^{n} SD_i^- \frac{\rho_{ns}}{\rho_w} EC_{eq} \right) \Big/ d \tag{6}$$

Where SD^- is the absolute change in SD (mm) when it decreases, *i* is the number of day during the snow season and *n* is the number of days since the start of the snow layer, ρ_{ns} and ρ_w are the density of new snow (100 kg m^{-3}) (Helfricht, et al., 2018) and liquid water (1000 kg m^{-3}), respectively. Average EC_{eq} is thus the sum of EC_{eq} in the layer *d* plus the EC_{eq} that is in layer *d* from the ablated snow. Therefore, average EC_{eq} depends strongly on the choice of *d.* A representative *d* value of 4 mm was determined as explained below in section 3.3. With a value of *d,* $\overline{EC_{eq}}$ was estimated from the cumulative reduction in SD using eq. 6. When the change in SD is positive (i.e. SD^+) then $\overline{EC_{eq}} = EC_{eq}$. Days with no change in SD were very rare. When this did occur, however, the previous day EC concentration was used. Using $\overline{EC_{eq}}$ from equation 6 when SD is decreasing (SD^-), or the base case when SD is increasing, together with r_e from equation 1, gives x in equation 5. The spectrally

https://doi.org/10.5194/acp-2021-158
Preprint. Discussion started: 26 March 2021

Atmospheric Chemistry and Physics
Discussions

dependent y_{λ}, from equation 4, was weighted over the solar spectrum between 400 and 900 nm using Table 1 of Hulstrom et al. (1985) in order to get the broad band scaling factor y_b. The albedo of the snow containing LAP was then estimated by scaling a_p from eq. 2 with y_b, as

$$a = a_p y_b \tag{7}$$

3.3 Influence from ground albedo and adjustment of parameter d

The resulting albedo will depend on the choice of the parameter *d*, making it imperative to assign a *d* value that makes the overall difference between observed and estimated albedo a minimum. The observed albedo a_{obs} is compared to a for each day, and the sum of $(a_{obs}-a)^2$ was calculated over the two seasons. By testing different values for *d*, we aimed to find a value of *d* that minimizes this sum. The possible influence from the albedo of the ground (a_g) below the snow surface was also considered. In Figure 2, $(a_{obs}-a)^2$ is plotted as a function of SD, where a is calculated with d=4 mm. Two sets of data are included using either T_a or T_s to parameterize SSA and r_e (equations S2 and S3). At about SD=50 cm and less, there is some deviation in increased $(a_{obs}-a)^2$, whereas at SD <20 cm it becomes much more apparent. For this reason, SD>55cm data was selected to be used in determining the best value for parameter *d*.

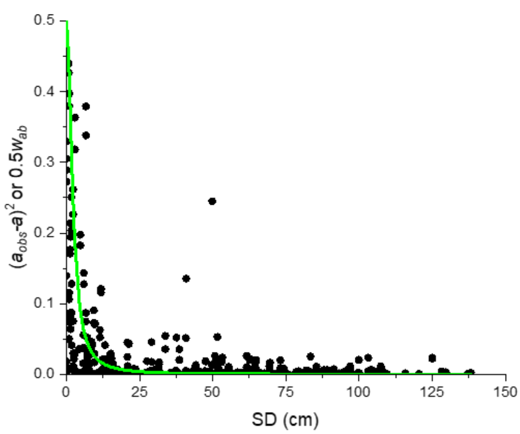

Figure 2. Presents the squared differences (dots) between observed albedo and the estimated albedo using SD changes and the air temperature or surface temperature as variables. For these calculations a *d* value of 4 mm was used. The green line is the weighting factor divided by 2, see text for details.

Figure 3 presents the variation in the sum of $(a_{obs}-a)^2$ for both seasons using both the T_a and T_s SSA fits, when SD>55 cm. The sums of errors are added for both seasons and both temperature parameterizations. As *d* increases, the sum decreases down to d=4 mm and then slowly increases again for larger *d*. Hence, a *d* value of 4 mm was selected. This parameter can be viewed as a numerical fix to other shortcomings in the assumptions above, but a physical interpretation of *d* is that it represents some e-folding thickness of the surface layer where

https://doi.org/10.5194/acp-2021-158
Preprint. Discussion started: 26 March 2021

LAP accumulates and interacts with radiation. Since this is expressed as mm SWE, the geometric thickness will depend on snow density. In its physical sense *d* is not a constant, but depends on the optical properties of the surface snow as well. For instance, a more transparent snow will allow the light to penetrate deeper for the same amount of SWE. This dependence is included to some extent through equation 5, where it is shown that the influence from LAP is enhanced with increasing grain size.

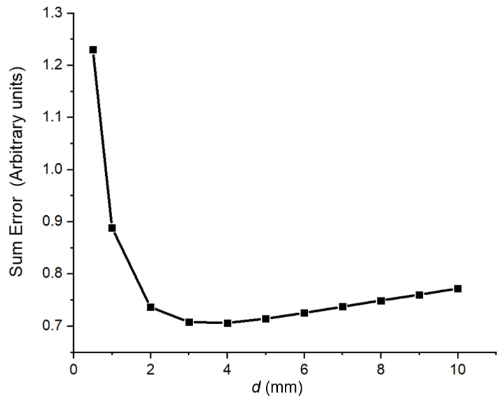

Figure 3. Sum of errors as function of the parameter *d*. Errors, $(a_{obs}-a)^2$, are added together for both seasons and both temperature parameterizations of equation S2 and S3. Only data where SD> 55 cm are included.

To accommodate the obvious influence from the ground albedo (a_g) for small SD, a simple mixing rule was introduced. The snow free a_g is taken as 0.17 (albedo of bare ground before and after snow seasons) which is weighted with *a* using a factor $w_{a_g} = f(SD)$. This function gives a weight of one at SD=0 cm and decreases towards zero as SD increases. The functional dependence of f(SD) is $1/\left(1+\frac{SD^2}{5}\right)$ and presented in Figure 2. As will be evident below (c.f Figure 4), the influence from a_g to albedo is only important at the very start and towards the end of the seasons. This weighting function helps in interpreting the results at either end of the seasons, but will not be of great importance for the remainder of the analysis. Therefore, no particular effort to adjust or motivate its shape will be performed. Nevertheless, the final estimated albedo is;

$$albedo = a\left(1-w_{a_g}\right) + a_g w_{a_g} \quad (8)$$

3.4 Comparison between observed and parameterized albedo

The observed albedo is compared to different parameterized albedos for the two seasons in Figure 4a-b. As expected, the pristine albedo (a_p), indicated by green line, is generally higher than the observed albedo (black line). The pristine albedo does, however, capture the seasonal albedo progression with increase and decrease events fairly well. Shown in Figure 4 is the pristine albedo based on T_a, only because the one derived from T_s is essentially identical. Once the LAP are taken into account using the base case of EC_{eq}=100 ng g^{-1} and *d*=4 mm, presented in red and blue lines (red utilizes T_a, while blue T_s in the albedo calculations), the observed albedo is closer matched. In both of these estimates the ground albedo is taken into account. For comparison, a purple

https://doi.org/10.5194/acp-2021-158
Preprint. Discussion started: 26 March 2021

line is also displayed to illustrate where the ground albedo (w_{ag} factor) is not taken into account for the albedo calculation. Thus, during periods where the purple line deviates from the red line the ground mainly influences the snow albedo, observed in the beginning and at the end of the study periods.

In summary, our results indicate that much of the observed variability in the snow albedo can be reproduced by using only two parameters, T_a and SD. The Pearson correlation coefficient between the observed albedo and $a(T_a)$ including w_{ag} for the two seasons put together is r^2=0.71, while when $a(T_s)$ is used r^2=0.77 (see Fig. S3).

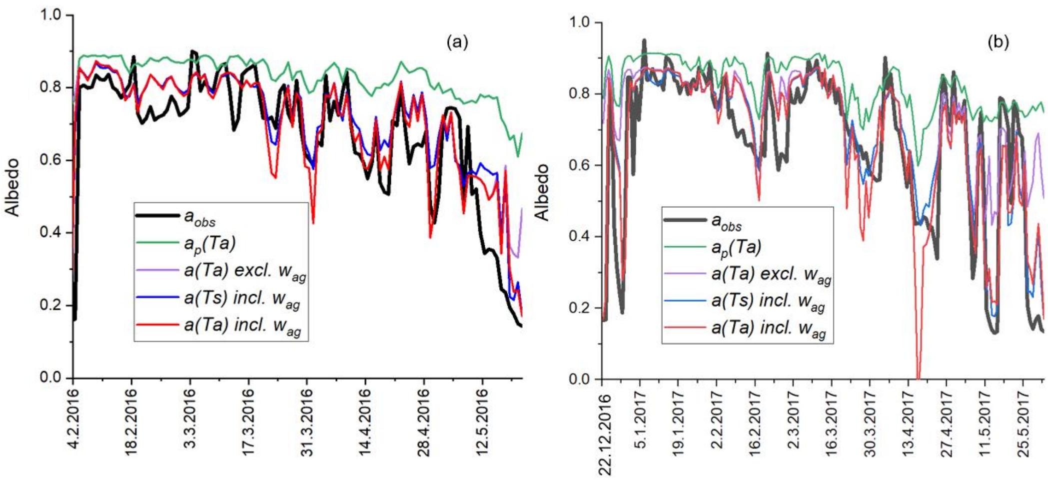

Figure 4. The observed albedo and emulated albedo using T_a or T_s with and without LAP and the influence from the underlying surface. Season 1 is presented in panel a), and season 2 is presented in panel b).

4. Radiative forcing by LAP through the reduction of snow albedo

4.1 Relative contribution to net SW radiation due to LAP

In this section the cumulative net SW radiation based on the observed incoming and reflected radiation is compared to parameterized cases using different EC_{eq} concentrations. The results are presented in Figure 5a and 5b for season 1 and season 2, respectively. It is evident that some of the difference between the observed net SW fluxes and the calculated net SW fluxes estimated based on different EC_{eq} concentrations is manifested already in the beginning of the seasons. This is a period when the sensitivity of net SW radiation to changes in LAP is small. This difference is interpreted as mainly a shortcoming in our simple diagnostic relation eq. 3 to capture the metamorphism of the snow. Because the incoming radiation is low at the start of the seasons, the cumulative effect on the available SW is less than during to the rest of the period. Nonetheless, the seasonal progression is displayed in each season, with the accumulation of LAP throughout the seasons and the subsequent increase in the calculated net SW fluxes. At the end of each season, our base case scenarios are broadly in line with the observed net SW fluxes.

https://doi.org/10.5194/acp-2021-158
Preprint. Discussion started: 26 March 2021

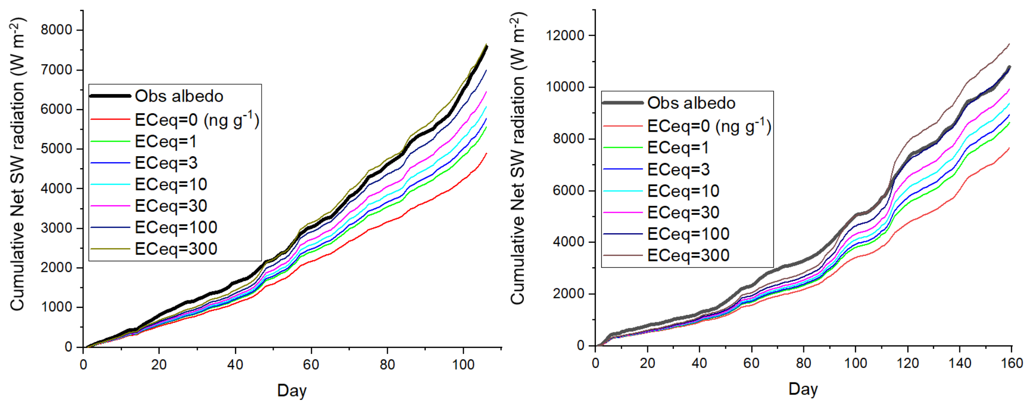

Figure 5. Cumulative net short wave radiation as a function of daily averaged SW_d calculated based on observed albedo (Obs albedo), and albedo from parameterizations using different values of EC_{eq}. Season 1 and season 2 are presented in panels a) and b), respectively.

Based on the endpoints in Figure 5a and 5b, the relative contribution from LAP to net SW radiation at the end of the season was calculated as function of EC_{eq}. The results are presented in Figure 6. As EC_{eq} increases, the relative contribution increases. Our base case of EC_{eq} concentration (100 ng g^{-1}) corresponds to slightly below 30% of extra energy accumulated over the entire season for both 1 and 2.

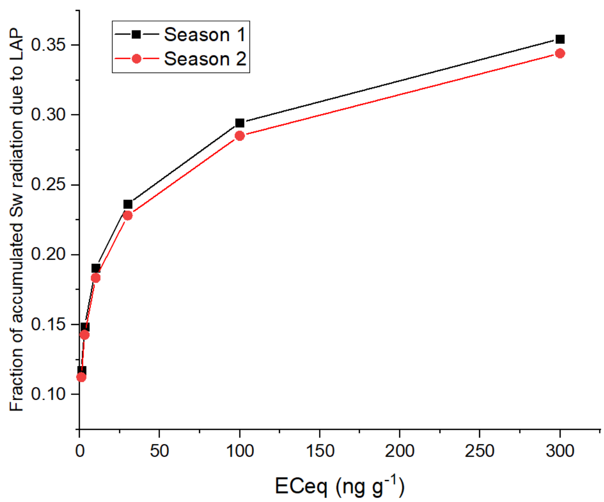

Figure 6. Fractional contribution to net SW radiation reaching the snow as function of EC_{eq} values. Data consists of the end points given in Figure 5.

4.2 Melt days

All of the extra energy accumulated over the season due to LAP is not available to melt the snow, as a large portion of the incoming energy is returned to the atmosphere as long wave radiation and latent heat. Conceptually, the snow pack increases its black body temperature to compensate for the incoming energy and

https://doi.org/10.5194/acp-2021-158
Preprint. Discussion started: 26 March 2021

this temperature increase will to some extent also increase the latent heat flux due to a larger vapor pressure gradient, and at the same time reduce the sensible heat flux due to decreasing temperature gradient. However, this temperature compensation can only continue until some critical temperature is reached and after that the excess energy is used to melt snow. Obviously, 0 °C would constitute such melt threshold and a common method to estimate melt is through the positive degree-day (PDD) concept (e.g. Braithwaite, 1995). The PDD models are formulated in their simplest form as,

$$M = DDF\ PDD \tag{9}$$

where PDD is the sum of daily mean air temperatures above the melting point, and M is the melt (mm, SWE) over the period of interest, and DDF is the degree-day factor (mm d^{-1} $^{o}C^{-1}$).

With knowledge on the seasonal M, we can compare the scaling factor, DDF, for our two seasons. This is determined by subtracting the loss of snow due to sublimation from PP, which is done by integrating the latent heat flux (LE) over the season and converting this energy into corresponding amount of SWE using the heat of sublimation (2.848 kJ kg^{-1}). The estimation of latent heat flux is presented in the supplement. For season 1 and season 2 the integrated LE losses are equivalent to 46 and 69 mm, respectively. The uncertainties in these values are high due to the simplified estimates of turbulent fluxes. However, they compare well to another study by Stigter et al. (2018), and constitute on average 0.43 and 0.42 mm d^{-1} loss of water to the atmosphere over the time for the seasonal snow cover. Using these estimates of LE, the derived DDF's are 10 (mm d^{-1} $^{o}C^{-1}$) for season 1, and 11 (mm d^{-1} $^{o}C^{-1}$) for season 2. Compared to other reported values for snow these estimates are high, but are close to those reported for ice (c.f. table 1 of Zhang et al., 2006). A summary of pertinent variables is summarized in Table 1. The number of days with snowmelt using this PDD concept is simply the number of days with an average air temperature above zero. For season 1 this is 14 days and for season 2 this is 26 days. Although the PDD concept indicates a consistency between the two seasons, it provides no direct linkage between the changes in LAP forcing and the air temperature.

On the other hand, T_s can be viewed as the response to changes in the energy fluxes. For this, we will explore how the net energy flux changes as function of the black body temperature, T_s to resolve at what threshold temperature the surplus energy is no longer compensated for and is instead available to melt the snow? To investigate this threshold, we combined the observed radiation fluxes and calculated turbulent latent and sensible heat fluxes into their daily net energy fluxes. These four fluxes are presented in Figure 7 as averages over one degree T_s bins. Temperatures above zero are grouped in the 0 °C bin. Warm precipitation, cold content, and geothermic flux are not considered, since all of those are expected to be comparably insignificant at our study case. Similar to the latent heat flux, an estimate of sensible heat flux is presented in supplement section 6.

https://doi.org/10.5194/acp-2021-158
Preprint. Discussion started: 26 March 2021

Atmospheric Chemistry and Physics
Discussions

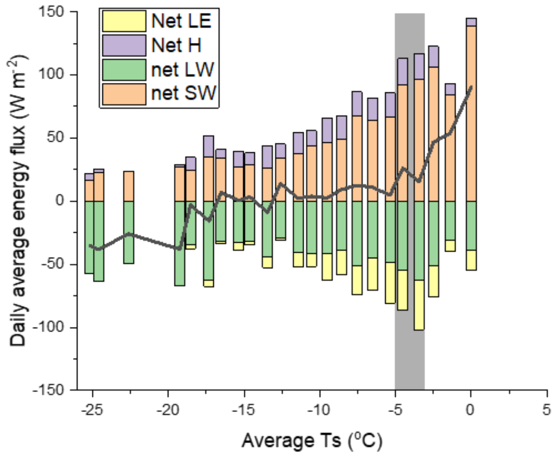

Figure 7. The major average energy fluxes for the combined data of Season 1 and Season 2. The black line is the average net flux for each temperature bin. The gray area marks the temperature range -5 to -3 ^{o}C.

The average net total energy flux for each degree interval of the black body temperature is overlaid the individual fluxes in Figure 7. It is worth noting that the absolute value of this total net flux is uncertain, but our interest is in its variation as a function of T_s. At very cold temperatures below -19 ^{o}C (few data points c.f. Fig. S2) there is a large deficit in the net budget, while at less cold temperatures up to about -5 ^{o}C the energy budget is nearly balanced. In the range -5 to -3 ^{o}C there is a shift in the tendency and the net energy surplus increases more rapidly. This shift in net energy as function of T_s we interpret as the conditions when the snowpack no longer fully compensates for the additional available energy and the snow starts melting. Days when T_s is greater than this threshold is defined as days when snowmelt occurs. A temperature of -4 ^{o}C will be used as our threshold value and -5 and -3 ^{o}C as our range of uncertainty.

Counting the days with $T_s > -4$ (-5, -3) ^{o}C, gives 27 (37,19) and 45 (56, 32) days for the respective seasons. This is about twice the number of days compared with using $T_a>0$ ^{o}C as criteria. The number of days with snowmelt (#SM) depend on the total amount of precipitation (PP), less the amount of water that is lost from net latent heat transport to the atmosphere (S). Noteworthy from Table 1, is that the fractions of estimated net S of PP are 0.16 and 0.15 for season 1 and season 2, respectively. Based on the comparable small fractions and the similarity between seasons, we assume that number of melt days can directly be compared to PP rather than (PP-S) if S can be described as a single factor multiplied by PP. Dividing our #SM estimates in Table 1 by the PP yields a #SM per mm PP. The resulting numbers for the two seasons are 0.093 and 0.098 d mm^{-1} using $T_s>-4$ ^{o}C.

Table 1

	Day	PP (mm)	Net Sublimation S (mm)	Fraction S/PP	$\#SM^{+\Delta\#SM}_{-\Delta\#SM}$ $T_s > -4^{(-5,-4)}_{(-4,-3)}{}^{\circ}C$	#SM/PP	Enhanced melt rate by LAP (mm d^{-1})

https://doi.org/10.5194/acp-2021-158
Preprint. Discussion started: 26 March 2021

Season 1	106	290	47	0.16	27^{10}_{8}	$0.093^{0.034}_{0.028}$	2.89
Season 2	159	460	69	0.15	45^{11}_{13}	$0.098^{0.024}_{0.028}$	2.18

The final step is to estimate the reduction in #SM due to LAP. This was achieved by comparing the accumulated amount of SW energy over the melt days only, using a range of EC_{eq} values. This is analogous to the presentation in Figure 6, but taking into account only those days when T_s is above threshold temperature. The respective LAP contributions are scaled by the #SM/PP factors in Table 1, yielding the estimated contribution to #SM ($\#SM_{LAP}$) as function of characteristic EC_{eq} in young snow and the seasonal precipitation. These data are presented in Figure 8 as the reduction in number of days with snowmelt per mm^{-1} as function of EC_{eq}.

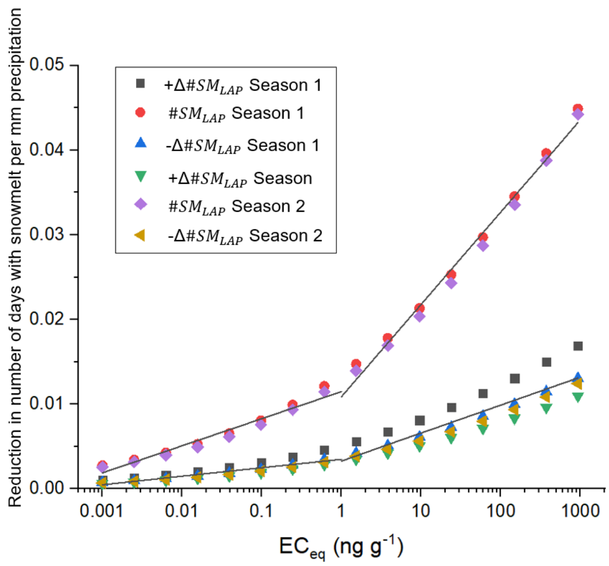

Figure 8. The reduction in number of days with snowmelt per mm seasonal precipitation as function of EC_{eq} concentration in young snow. The straight lines represent the relations in equations 10 through 13, see text for details.

The upper and lower range in $\#SM_{LAP}$ for each season, based on T_s, are presented as $\pm\Delta\#SM_{LAP}$. The dependence of the contribution to #SM on (EC_{eq}) is non-linear, but dividing the concentration above and below about 1 ng g^{-1}, reasonable agreement can still be achieved using linear fits and $\log(EC_{eq})$. The four equations multiplied with PP then become:

For EC_{eq} > 1ng g^{-1}

$$\#SM_{LAP} = 0.0109\left(log\left(EC_{eq}\right) + 1\right)PP \tag{10}$$

$$\pm\Delta\#SM_{LAP} = 0.0033(\log\left(EC_{eq}\right) + 1)PP \tag{11}$$

For $EC_{eq} \leq 1$ ng g-1

$$\#SM_{LAP} = \left(0.0032log\left(EC_{eq}\right) + 0.0115\right)PP \tag{12}$$

https://doi.org/10.5194/acp-2021-158
Preprint. Discussion started: 26 March 2021

Atmospheric Chemistry and Physics Discussions

$$\pm\Delta\#SM_{LAP} = \left(0.001log\left(EC_{eq}\right) + 0.0035\right)PP \tag{13}$$

Assuming a constant melt rate of the melting period the #SM can be expressed as melt rate. Without the influence of LAP, season 1 would have 27 plus 14 (from eq. 10) days with melting, which yields to total of (290-47)/(27+14)=6.11 mm of snowmelt per day. Taking into account the influence of LAP we obtain (290-47)/27=9 mm per day. This means 2.89 mm extra melt due to LAP. Analogous to this, for season 2 we get 2.18 mm per day in extra melt due to LAP.

5. *Discussion and conclusions*

Based on AWS data and an important assumption of a constant LAP deposition, a set of very simplified equations (10-13) to calculate the shift in snow melt-out date were derived. To arrive at these equations, a first step consisted of displaying that the observed daily variation in albedo could be emulated based on the assumption about constant LAP deposition and only two other variables from the AWS, namely air temperature and snow depth. The follow-up step involved the analysis of the energy balance and temperature response of the snow layer in order to define the period of days with melting snow. By combining the information from this sequence the potential contribution from LAP to the #SM be estimated based on the LAP content and amount of precipitation. With a numerical example using our base case of EC_{eq}=100 ng g^{-1} and a PP of 400 mm gives an advancement of the melt-out date of 13 days ±4 days (using equations 10 and 11). Because the inversion of DDF includes the contribution from LAP implicitly, this large shift in the #SM used in the PDD concept led to an overestimation of the melting compared to pristine snow.

The response in the #SM from changes in LAP is less for very clean snow compared to snow with higher EC_{eq}, as is visible in the changed slope that occurs around EC_{eq}=1 ng g^{-1} (Fig. 8). For clean snow conditions the reduction is only about 1 day for every 100 mm of precipitate near the 1 ng g^{-1} intercept. This result suggests that the enhanced melt of seasonal snow cover due to LAP in very clean regions is not very important. When comparing with the shape of the relation in Figure 6, which indicate a very rapid increase in the fraction of energy for small EC_{eq}, this may seem a little contradictive. A plausible explanation is that much of the reduction in albedo during the melt period is from the metamorphism of the snow itself, masking the contribution from LAP, however. This highlights the important insight that LAP can really enhance melting only during the melt period, as previously reported (e.g. Flanner et al., 2007; Jacobi et al., 2015).Our simplistic approach does not take into account all feedback mechanisms, for instance, that LAP enhance snow grain growth. The effect of LAP may in turn be underestimated. Nevertheless, from Figure 4 and 5 it shows that albedo and energy fluxes are reasonable well emulated.

The main objective of this study was to address the #SM to changes in LAP. From equation 10 this can be expressed in very general terms. For each doubling of EC_{eq} the melt period is shortened by $0.0109log(2)PP$ or about $\frac{1}{3}$ of a day per 100 mm precipitation. For our base case EC_{eq} =100 ng g^{-1} and 400 mm precipitation, changing EC_{eq} by a factor two up or down will change the #SM by about $1\frac{1}{3}$ days forward or backward. Changing

https://doi.org/10.5194/acp-2021-158
Preprint. Discussion started: 26 March 2021

the LAP content by a factor of two constitute a rather large change if we consider that about half of the LAP was of natural origin through contribution of MD (for the observation site).

In the scenario set up for our study region, a large change in anthropogenic deposition is required to achieve a sizeable change in the #SM due to the large background forcing by MD. However, the contribution by EC alone to snowmelt is not small. A shift in the #SM due to half the base case EC_{eq} (with half of the base case constituting representable EC content in the snow at this site) is still 13 days assuming a PP=400mm. Assuming a constant natural MD contribution, a threefold change in anthropogenic EC would be required to increase EC_{eq} a factor of two. Our numerical estimates of the $\#SM_{LAP}$ are broadly in the same range with those reported previously for the Himalaya (e.g. Ménégoz et al., 2014; Zhang et al., 2018; Zhong et al. 2019). In addition, our method allows to estimate the LAP impact on the #SM in a more general form, given that the amount of precipitation and LAP mean deposition are known.

On a broader geographical scale, beyond the Himalaya, our results compare well with studies investigating the reduction in snow cover due to LAP in other areas. In the European Alps, Tuzet et al. (2020), estimated a 10±5 and 11±1 day shortening of two separate snow seasons in the French Alps using a combination of extensive in-situ observations and process models. Similarly, in the Italian Alps, Di Mauro et al. (2019), reported on an exceptional year with strong MD deposition with LAP advancing the seasonal snow melt by 38 days out of a total 7 months of typical snow duration. This highlights the importance in assessing the anthropogenic influence on the reduction of snow cover duration to further investigate the relative role between EC and MD. An even stronger impact by MD has been estimated for Rocky Mountain snow, Colorado, US (Skiles et al., 2012). For that site the authors suggested as much as a 51 day advancement of the MOD attributed to MD primarily.

https://doi.org/10.5194/acp-2021-158
Preprint. Discussion started: 26 March 2021

Data availability

All data are available upon request.

Author contributions

JSv, HH, EA, NBD, and HL participated in the collection of field measurements. JSt and JSv analyzed the data and wrote the paper. ST, RH, VPS, ML, HL, and AH took care of project administration. HH, EA, RH, OM, H-WJ, ML,HL, and AH helped with the interpretation of the data. All authors agreed on the content of the paper.

Competing interests

The authors declare that they have no conflict of interest.

Acknowledgments

This work has been supported by the Academy of Finland project: Absorbing Aerosols and Fate of Indian Glaciers (AAFIG; project number 268004), and the Academy of Finland consortium: "Novel Assessment of Black Carbon in the Eurasian Arctic: From Historical Concentrations and Sources to Future Climate Impacts" (NABCEA project number 296302), and the Academy of Finland Flagship (grant no. 337552). JSt is part of the Bolin Centre for Climate Research, and acknowledges the Swedish Research Council grant 2017-03758. JSv acknowledges support from the two foundations Maj and Tor Nessling and Oskar Huttunen, as well as the invited scientist grant from the UGA.

https://doi.org/10.5194/acp-2021-158
Preprint. Discussion started: 26 March 2021

Atmospheric Chemistry and Physics Discussions

References

Aoki, T., Hachikubo, A., and Hori, M.: Effects of snow physical parameters on shortwave broadband albedos, J. Geophys. Res., 108, 4616, doi:10.1029/2003JD003506, 2003.

Armstrong, R. L., Rittger, K., Brodzik, M. J., Racoviteanu, A., Barrett, A. P., Khalsa, S.-J. S., Raup, B., Hill, A. F., Khan, A. L., Wilson, A. M., Kayastha, R. B., Fetterer, F., and Armstrong, B.: Runoff from glacier ice and seasonal snow in High Asia: separating melt water sources in river flow, Reg. Environ. Chang., 19, 1249–1261, doi.org/10.1007/s10113-018-1429-0, 2019.

Bonasoni, P., Laj, P., Marinoni, A., Sprenger, M., Angelini, F., Arduini, J., Bonafè, U., Calzolari, F., Colombo, T., Decesari, S., Di Biagio, C., di Sarra, A. G., Evangelisti, F., Duchi, R., Facchini, MC., Fuzzi, S., Gobbi, G. P., Maione, M., Panday, A., Roccato, F., Sellegri, K., Venzac, H., Verza, G. P., Villani, P., Vuillermoz, E., and Cristofanelli, P.: Atmospheric Brown Clouds in the Himalayas: first two years of continuous observations at the Nepal Climate Observatory-Pyramid (5079 m), Atmos. Chem. Phys., 10, 7515–7531, doi:10.5194/acp-10-7515-2010, 2010.

Braithwaite, R., Positive degree-day factors for ablation on the Greenland ice sheet studied by energy-balance modelling. J. Glacio., 41, 153-160, 1995.

Brock, B.W:, Willis, I.C., Sharp, M.J., Measurement and parameterization of albedo variations at Haut Glacier d'Arolla, Switzerland, J. Glaciol, 46, 675-688, 2000.

Colbeck, S. C.: Grain clusters in wet snow, J. Colloid Interface Sci., 72(3), 371– 384, doi.org/10.1016/0021-9797(79)90340-0, 1979.

Cuffey, K. and Paterson, W. S. B.: The Physics of Glaciers, Elsevier, Butterworth-Heineman, Burlington, MA, USA, 2010.

Di Mauro, B., Garzonio, R., Rossini, M., Filippa, G., Pogliotti, P., Galvagno, M., Morra di Cella, U., Migliavacca, M., Baccolo, G., Clemenza, M., Delmonte, B., Maggi, V., Dumont, M., Tuzet, F., Lafaysse, M., Morin, S., Cremonese, E., and Colombo, R.: Saharan dust events in the European Alps: role in snowmelt and geochemical characterization, Cryosphere, 13, 1147–1165, doi.org/10.5194/tc-13-1147-2019, 2019.

Doherty, S. J., Grenfell, T. C., Forsström, S., Hegg, D. L., Brandt, R. E., and Warren, S. G.: Observed vertical redistribution of black carbon and other insoluble light-absorbing particles in melting snow, J. Geophys. Res., 118, 1–17, doi.org/10.1002/jgrd.50235, 2013.

Emerson, E. W., Katich, J. M., Schwarz, J. P., McMeeking, G. R., and Farmer, D. K.: Direct Measurements of Dry and Wet Deposition of Black Carbon Over a Grassland, J. Geophys. Res.-Atmos., 123, 12277–212290, doi.org/10.1029/2018JD028954, 2018.

Flanner, M. G., Zender, C. S., Randerson, J. T., and Rasch, P. J.: Present-day climate forcing and response from black carbon in snow, J. Geophys. Res.-Atmos., 112, D11202, doi.org/10.1029/2006JD008003, 2007.

Forsström, S., Ström, J., Pedersen, C. A., Isaksson, E., and Gerland, S.: Elemental carbon distribution in Svalbard snow, J. Geophys. Res.-Atmos., 114, D19112, doi.org/10.1029/2008JD011480, 2009.

Gardner, A. S. and Sharp, M. J.: A review of snow and ice albedo and the development of a new physically based broadband albedo parameterization, J. Geophys. Res., 115, F01009, doi:10.1029/2009JF001444, 2010.

Gertler, C. G., Puppala, S. P., Panday, A., Stumm, D., and Shea, J.: Black carbon and the Himalayan cryosphere: A review, Atmos. Environ., 125, 404–417, doi.org/10.1016/j.atmosenv.2015.08.078, 2016.

Helfricht, K., Hartl, L., Koch, R., Marty, C., and Olefs, M.: Obtaining sub-daily new snow density from automated measurements in high mountain regions, Hydrol. Earth Syst. Sci., 22, 2655–2668, doi.org/10.5194/hess-22-2655-2018, 2018.

https://doi.org/10.5194/acp-2021-158
Preprint. Discussion started: 26 March 2021

Hulstrom, R., Bird, R., Riordan, C., Spectral solar irradiance data sets for selected terrestrial conditions. Solar Cells, 15, 365-391, 1985.

Jacobi, H.-W., Lim, S., Ménégoz, M., Ginot, P., Laj, P., Bonasoni, P., Stocchi, P., Marinoni, A., and Arnaud, Y.: Black carbon in snow in the upper Himalayan Khumbu Valley, Nepal: observations and modeling of the impact on snow albedo, melting, and radiative forcing, Cryosphere, 9, 1685–1699, doi.org/10.5194/tc-9-1685-2015, 2015.

Ménégoz, M., Krinner, G., Balkanski, Y., Boucher, O., Cozic, A., Lim, S., Ginot, P., Laj, P., Gallée, H., Wagnon, P., Marinoni, A., and Jacobi, H. W.: Snow cover sensitivity to black carbon deposition in the Himalayas: from atmospheric and ice core measurements to regional climate simulations, Atmos. Chem. Phys., 14, 4237–4249, doi.org/10.5194/acp-14-4237-2014, 2014.

Mimeau, L., Esteves, M., Zin, I., Jacobi, H.-W., Brun, F., Wagnon, P., Koirala, D., and Arnaud, Y.: Quantification of different flow components in a high-altitude glacierized catchment (Dudh Koshi, Himalaya): some cryospheric-related issues, Hydrol. Earth Syst. Sci., 23, 3969–3996, doi.org/10.5194/hess-23-3969-2019, 2019.

Ming, J., Cachier, H., Xiao, C., Qin, D., Kang, S., Hou, S., and Xu, J.: Black carbon record based on a shallow Himalayan ice core and its climatic implications, Atmos. Chem. Phys., 8, 1343–1352, doi:10.5194/acp-8-1343-2008, 2008.

Pedersen, C. A., Gallet, J.-C, Ström, J., Gerland, S., Hudson, S. R., Forsström, S., Isaksson, E., and T. K. Berntsen, T.K.: In situ observations of black carbon in snow and the corresponding spectral surface albedo reduction, J. Geophys. Res. Atmos., 120, 1476–1489, doi:10.1002/2014JD022407, 2015.

Petzold, A., Ogren, J. A., Fiebig, M., Laj, P., Li, S.-M., Baltensperger, U., Holzer-Popp, T., Kinne, S., Pappalardo, G., Sugimoto, N., Wehrli, C., Wiedensohler, A., and Zhang, X.-Y.: Recommendations for reporting "black carbon" measurements, Atmos. Chem. Phys., 13, 8365–8379, doi.org/10.5194/acp-13-8365-2013, 2013.

Sarangi, C., Qian, Y., Rittger, K., Leung, R., Chand, D., Bormann, K. J., Painter, T. H.: Dust dominates high-altitude snow darkening and melt over high-mountain Asia. Nat. Clim. Chang. 10, 1045–1051, doi.org/10.1038/s41558-020-00909-3, 2020.

Schmale, J, Flanner, M., Kang, S., Sprenger, M., Zhang, Q., Guo, J., Li, Y., Schwikowski, M., Farinotti, D., Modulation of snow reflectance and snowmelt from Central Asian glaciers by anthropogenic black carbon Sci. Rep. 7, 40501; doi: 10.1038/srep40501, 2017.

Schwarz, J. P., Doherty, S. J., Li, F., Ruggiero, S. T., Tanner, C. E., Perring, A. E., Gao, R. S., and Fahey, D. W.: Assessing Single Particle Soot Photometer and Integrating Sphere/Integrating Sandwich Spectrophotometer measurement techniques for quantifying black carbon concentration in snow, Atmos. Meas. Tech., 5, 2581–2592, doi.org/10.5194/amt-5-2581-2012, 2012.

Skiles, S. M., Painter, T. H., Deems, J., Landry, C. & Bryant, A.: Dust radiative forcing in snow of the Upper Colorado River Basin. Part II: interannual variability in radiative forcing and snowmelt rates. Water Resour. Res. 48, W07522, 2012.

Stigter, E. E., Maxime Litt, A., Jakob Steiner, F., Pleun Bonekamp, N. J., Joseph Shea, M., and Immerzeel, W. W.: The importance of snow sublimation on a himalayan glacier. Front. Earth Sci. 6:108, doi: 10.3389/feart.2018.00108, 2018.

Svensson J., Virkkula A., Meinander O., Kivekäs N., Hannula H.-R., Järvinen O., Peltoniemi J.I., Gritsevich M., Heikkilä A., Kontu A., Neitola K., Brus D., Dagsson-Waldhauserova P., Anttila K., Vehkamäki M., Hienola A., de Leeuw G. & Lihavainen H.: Soot-doped natural snow and its albedo — results from field experiments. Boreal Env. Res. 21: 481–503, 2016.

https://doi.org/10.5194/acp-2021-158
Preprint. Discussion started: 26 March 2021

Atmospheric Chemistry and Physics
Open Access
EGU
Discussions

Svensson, J., Ström, J., Kivekäs, N., Dkhar, N. B., Tayal, S., Sharma, V. P., Jutila, A., Backman, J., Virkkula, A., Ruppel, M., Hyvärinen, A., Kontu, A., Hannula, H.-R., Leppäranta, M., Hooda, R. K., Korhola, A., Asmi, E., and Lihavainen, H.: Light-absorption of dust and elemental carbon in snow in the Indian Himalayas and the Finnish Arctic, Atmos. Meas. Tech., 11, 1403–1416, doi.org/10.5194/amt-11-1403-2018, 2018.

Svensson, J., Ström, J., Honkonen, H., Asmi, E., Dkhar, N. B., Tayal, S., Sharma, V. P., Hooda, R., Leppäranta, M., Jacobi, H.-W., Lihavainen, H., and Hyvärinen, A.: Deposition of light-absorbing particles in glacier snow of the Sunderdhunga Valley, the southern forefront of Central Himalaya, Atmos. Chem. Phys. Discuss., doi.org/10.5194/acp-2020-1059, accepted, 2021.

Tuzet, F., Dumont, M., Picard, G., Lamare, M., Voisin, D., Nabat, P., Lafaysse, M., Larue, F., Revuelto, J., and Arnaud, L.: Quantification of the radiative impact of light-absorbing particles during two contrasted snow seasons at Col du Lautaret (2058 m a.s.l., French Alps), Cryosphere, 14, 4553–4579, doi.org/10.5194/tc-14-4553-2020, 2020.

Warren, S. and Wiscombe, W.: A model for the spectral albedo of snow II. Snow containing atmospheric aerosols, J. Atmos. Sci., 37, 2734–2745, 1980.

Winter, J.-G., Short- and long-term variability of snow albedo, Nord. Hydrol., 24, 199-212, 1993.

Xu, B., Cao, J., Joswiak, D.R., Liu, X., Zhao, H., He, J., Zhang, Y., Shiyin, L., Yongjian, D.: Post-depositional enrichment of black soot in snow-pack and accelerated melting of Tibetan glaciers, Environ. Res. Lett., 7, doi:10.1088/1748-9326/7/1/014022, 2012.

Zhang, Y., Shiyin, L., Yongjian, D., Observed degree-day factors and their spatial variations on glaciers in western China. Ann. Glaciol., 43, 301-306, 2006.

Zhang, Y., Kang, S., Sprenger, M., Cong, Z., Gao, T., Li, C., Tao, S., Li, X., Zhong, X., Xu, M., Meng, W., Neupane, B., Qin, X., and Sillanpää, M.: Black carbon and mineral dust in snow cover on the Tibetan Plateau, Cryosphere, 12, 413–431, doi.org/10.5194/tc-12-413-2018, 2018.

Zhong X, Kang S, Zhang W, Yang J, Li X, Zhang Y, Liu Y, Chen P.: Light-absorbing impurities in snow cover across Northern Xinjiang, China, J. Glaciol., 1-18, doi.org/10.1017/jog.2019.69, 2019.

https://doi.org/10.5194/acp-2021-158
Preprint. Discussion started: 26 March 2021

Atmospheric Chemistry and Physics Discussions

Symbols and acronyms

a	Estimated broad band albedo
a_{obs}	Observed broad band albedo
a_p	Broad band albedo of pristine snow
a_g	Broad band albedo of snow free ground
AWS	Automatic weather station
BC	Black carbon
BrC	Brown carbon
d	Characteristic depth of surface snow
DDF	Degree-day factor
EC_{eq}	Elemental carbon equivalent
$\overline{EC_{eq}}$	Effective or average ECeq
H	Sensible heat flux
LAP	Light-absorbing particles
LE	Latent heat flux
LWu	Long wave radiation up
LWd	Long wave radiation down
PDD	Positive degree-day
PP	Precipitation
RH	Relative humidity
rBC	Refractory black carbon
Re	Effective radius
ρ_i	Density of ice
ρ_{ns}	Density of new snow
ρ_w	Density of water
S	Sublimation
SD	Snow depth
SD^-	Decreasing snow depth
SD^+	Increasing snow depth
#SM	Number of days with snowmelt
SSA	Specific surface area
SWE	Snow water equivalent
SWd	Short wave radiation down
SWu	Short wave radiation up
T_a	Air temperature

https://doi.org/10.5194/acp-2021-158
Preprint. Discussion started: 26 March 2021

Atmospheric Chemistry and Physics Discussions

T_s	Surface temperature
U	Wind speed
w_{a_g}	Weighting factor between a and a_g
y_λ	Spectral albedo reduction due to LAP
y_b	Broad band albedo reduction due to LAP